

Effect of fluorocarbon chains on the mesomorphic properties of chiral imines and their complexes with copper(II)[†]

Hale Ocak,^a Belkız Bilgin-Eran,^{*a} Carsten Tschierske,^b Ute Baumeister^c and Gerhard Pelzl^c

Received 12th March 2009, Accepted 26th June 2009

First published as an Advance Article on the web 5th August 2009

DOI: 10.1039/b905104j

The synthesis and mesomorphism of new chiral imine compounds incorporating a fluorocarbon chain which have calamitic molecular shape and their complexes with copper(II) are reported. The liquid crystalline properties were investigated using polarised optical microscopy, differential scanning calorimetry and X-ray diffraction. Imine compounds with a semifluorinated chain and a short chiral chain show chiral smectic mesophases with dramatically enhanced mesophase stabilities compared to the related hydrocarbon derivatives. In addition, the first examples of mesogenic chiral salicylaldimine copper(II) complexes carrying semifluorinated alkyl chains at their peripheries have been synthesized and their liquid crystalline properties were investigated.

1. Introduction

The introduction of fluorine and the choice of its position within liquid crystalline compounds allow the preparation of materials which have considerable technological interest for display and non-display applications.^{1–3} The combination of small size and high polarity of fluoro substituents permits the modification of the melting point, transition temperatures, mesophase type and a wide range of physical properties of liquid crystal materials.^{3–11} Fluorine atoms can replace H atoms at the rigid core or at the flexible chains. Usually, perfluorination of the terminal chains of rod-like molecules suppresses the formation of nematic phases and induces smectic ones. The main reason for this behaviour is the incompatibility of these chains with aromatic and aliphatic building blocks of the mesogenic molecules (nano-segregation, fluorophobic effect); the increased stiffness of perfluoroalkyl chains and steric effects due to the larger size of F compared to H are also important. Fluorinated chains can significantly influence the mode of organization and the specific properties of smectic phases, as for example they can lead to a strongly tilted organization with alternating tilt direction (orthoconic LC if the tilt angle is 45°)¹² or give rise to randomly tilted deVries type materials.¹³ Chiral rod-like liquid crystals are of interest as they can have ferroelectric or antiferroelectric properties which are also of interest for applications.¹⁴ Our group has reported a variety of fluorinated mesogens and studied the structure-property relationships in different molecular types;^{7–9} for example, fluorinated imine compounds and their metal complexes were investigated in depth.¹⁵

The work described herein deals with the synthesis and characterization of liquid crystalline properties of two types of new imines, **6** and **7**, combining a semifluorinated chain and a chiral alkyl chain. As these imine compounds possess the ability to coordinate to metals the first examples of mesogenic salicylaldimine derived copper(II) complexes¹⁶ combining chain fluorination and chirality are reported.

2. Results and discussion

2.1. Synthesis

The synthesis of the compounds is presented in Scheme 1. The chiral moiety was introduced by reaction of (*S*)-2-methylbutyltosylate¹⁷ (prepared from (*S*)-(-)-2-methyl-1-butanol, Fluka, 95.0%, $[\alpha]_D^{20} -6.3 \pm 0.5^\circ$, $c = 10$ in EtOH), with *p*-nitrophenol in DMF to give (*S*)-1-(2-methylbutoxy)-4-nitrobenzene (**2**) as described previously;^{17b} **2** was then reduced to the corresponding aniline **3**.

The semiperfluorinated aldehydes **4** and **5** were obtained by reaction of 2,4-dihydroxybenzaldehyde and 4-hydroxybenzaldehyde, respectively, with the appropriate semifluorinated alkyl bromides,¹¹ using KHCO₃ or K₂CO₃ as base and DMF as solvent.

The synthesis of the imine ligands **6** and **7** as well as the copper(II) complexes **8** is also outlined in Scheme 1. The condensation of the aldehydes **4**, **5** and (*S*)-4-(2-methylbutoxy)aniline in toluene with *p*-toluenesulfonic acid as catalyst gave the Schiff bases **6** and **7**. The copper complexes **8** were obtained by the reaction of the salicylaldimine ligands with copper(II) acetate dihydrate in ethanol (see the ESI[†]). Compounds **6a** and **7a** were first reported by Serrano *et al.*¹⁸ and have been included for comparison.

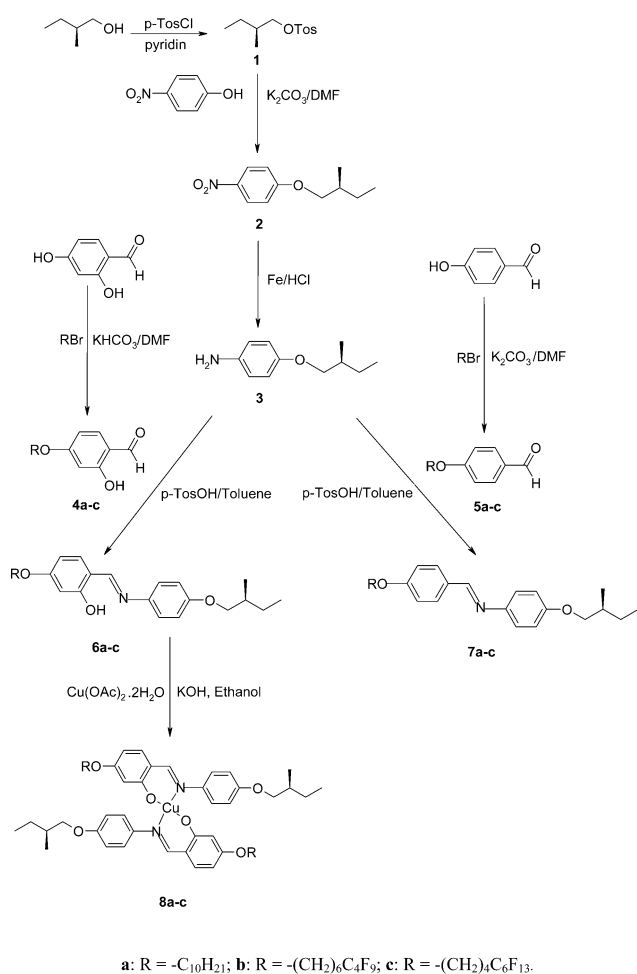
The imines **6** and **7** were characterized by the common spectroscopic methods (¹H-, ¹³C-NMR, UV-VIS, IR and MS) and by elemental analysis. The copper(II) complexes **8** were characterized by UV-VIS, IR and MS. The spectroscopic data of the materials are consistent with their proposed structures (see the ESI[†]).

^aDepartment of Chemistry, Yildiz Technical University, Davutpaşa Yerleşim Birimi, TR-34210 Esenler, Istanbul, Turkey

^bInstitute of Chemistry, Organic Chemistry, Martin-Luther University Halle-Wittenberg, Kurt Mothes-Str. 2, D-06120 Halle, Germany

^cInstitute of Chemistry, Physical Chemistry, Martin-Luther University Halle-Wittenberg, Mühlpforte 1, D-06118 Halle, Germany

[†] Electronic supplementary information (ESI) available: Experimental conditions for X-ray scattering and additional X-ray data; electrooptical investigations of **6c**; synthesis and analytical data. See DOI: 10.1039/b905104j



Scheme 1 Synthesis of the salicylaldimines **6a–c**, the imines **7a–c** and the salicylaldiminate Cu(II) complexes **8a–c**.

In the ¹H-NMR spectra the characteristic resonance of the imine protons of the salicylaldimines and the imines without ortho-hydroxyl group appeared at around 8.49 ppm and 8.38 ppm, respectively. These values are well within the range expected for imines. In the electronic spectra, the absorption band of the salicylaldimine ligands **6** is observed at around

349.0 nm, whereas the absorption bands of the complexes **8** is shifted to 381.0 nm. The imine compounds **7** without 2-hydroxyl group show the absorption band around 335 nm. The IR spectra of the salicylaldimine ligands **6** and their complexes **8** show the C=N stretching vibration at around 1615–1618 cm⁻¹ and 1610–1612 cm⁻¹, respectively. The frequency of the C=N stretching vibration of the starting salicylaldimines decreases by about 5–7 cm⁻¹ due to complex formation as also reported previously in similar studies.¹⁹ In addition, the C=N stretching band of the imines is **7** shifted to 1604–1607 cm⁻¹.

As the stereogenic center of (*S*)-(-)-2-methyl-1-butanol is not touched during the synthesis it can be assumed that the optical purity of the products corresponds to the starting material. An optical rotation of [α]_D²⁰ +11.8° (*c* = 0.4 in CHCl₃) was measured for compound **6c** as a representative example.

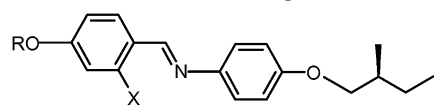
2.2. Liquid crystalline properties

The mesomorphic properties of the obtained two series of imines **6** and **7** and the copper(II) complexes **8** were investigated using polarised light optical microscopy (PM), differential scanning calorimetry (DSC) and some of them by X-ray diffraction. All of the salicylaldimines, their copper(II) complexes and the imines show thermotropic mesomorphic behaviour and exhibit smectic mesophases. The transition temperatures, corresponding enthalpy values and mesophase types observed for the compounds **6**, **7** and **8** are summarized in Tables 1 and 2, respectively.

Mesomorphic properties of salicylaldimine compounds 6. The imine **6a**, containing two peripheral alkyl chains (one alkyl chain and one short and branched chiral chain), exhibits a short range of a smectic A phase with fan-shaped texture and at lower temperature the fingerprint texture of a chiral smectic C* phase was observed. This is distinct from the phase sequence described previously,¹⁸ where enantiotropic SmC* and chiral nematic phases were reported (see Table 1).

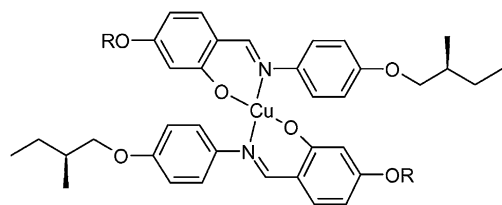
The chiral salicylaldimines **6b** and **6c**, containing fluorocarbon terminal chains, show chiral smectic mesophases. On cooling compounds **6b** and **6c** from the homeotropically aligned SmA phase the optically isotropic regions become birefringent and

Table 1 Phase transition temperatures and transition enthalpies of semifluorinated imine compounds **6** and **7**^a

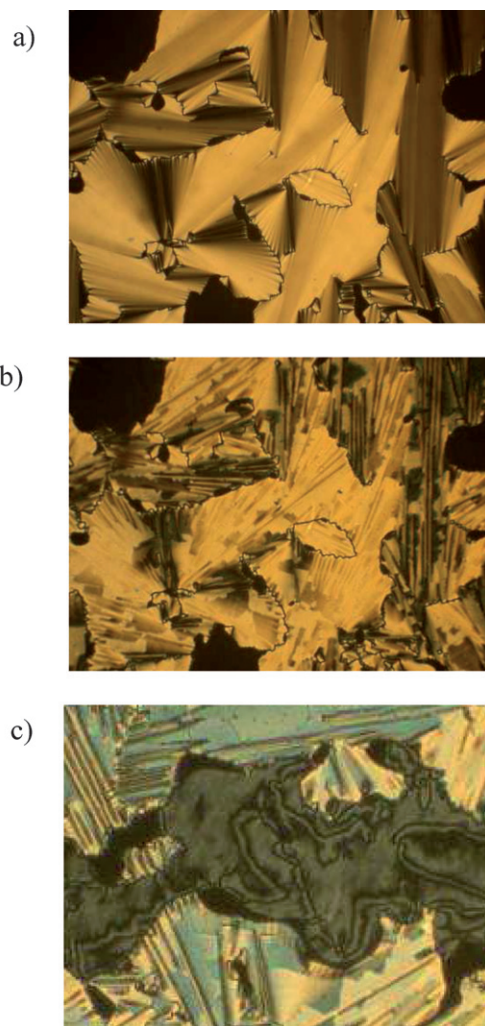


Compound	X	R	T ^o C [ΔH kJ/mol]
6a ^b	OH	-C ₁₀ H ₂₁	Cr 50 [25.0] SmC* 84 [0.9] SmA 86 [1.0] Iso
6b	OH	-(CH ₂) ₆ C ₄ F ₉	Cr 78 [24.7] SmC* 106 [0.1] SmA 146 [6.1] Iso
6c	OH	-(CH ₂) ₄ C ₆ F ₁₃	Cr 81 [15.0] SmC* 125 [0.2] SmA 175 [6.9] Iso
7a ^c	H	-C ₁₀ H ₂₁	Cr 90 [46.4] (SmC* 76 SmA 78 [4.9]) Iso
7b	H	-(CH ₂) ₆ C ₄ F ₉	Cr 101 [34.4] (SmC* 99 [0.3]) SmA 127 [4.5] Iso
7c	H	-(CH ₂) ₄ C ₆ F ₁₃	Cr 94 [28.3] (SmX* 70 [1.3]) SmC* 118 [0.2] SmA 142 [4.2] Iso

^a Perkin-Elmer DSC-7; heating rates 10 K min⁻¹; enthalpy values are given behind the phase transition temperatures in italics in square parentheses; abbreviations: Cr = crystalline, SmA = nontilted smectic phase, SmC* = chiral smectic C phase, SmX = low temperature mesophase with unknown structure and Iso = isotropic liquid phase; monotropic transitions are indicated by parentheses. ^b In ref. 18 for compound **6a**: Cr 50.7 [7.3] SmC* 86.2 [0.5] Ch* 88.2 [0.5] Iso. ^c In ref. 18 for compound **7a**: Cr 83.8 [10.6] (SmC* 79.5 SmA 81.2 [1.2]) Iso.

Table 2 Phase transition temperatures and transition enthalpies of semifluorinated copper(II) complexes **8**^a

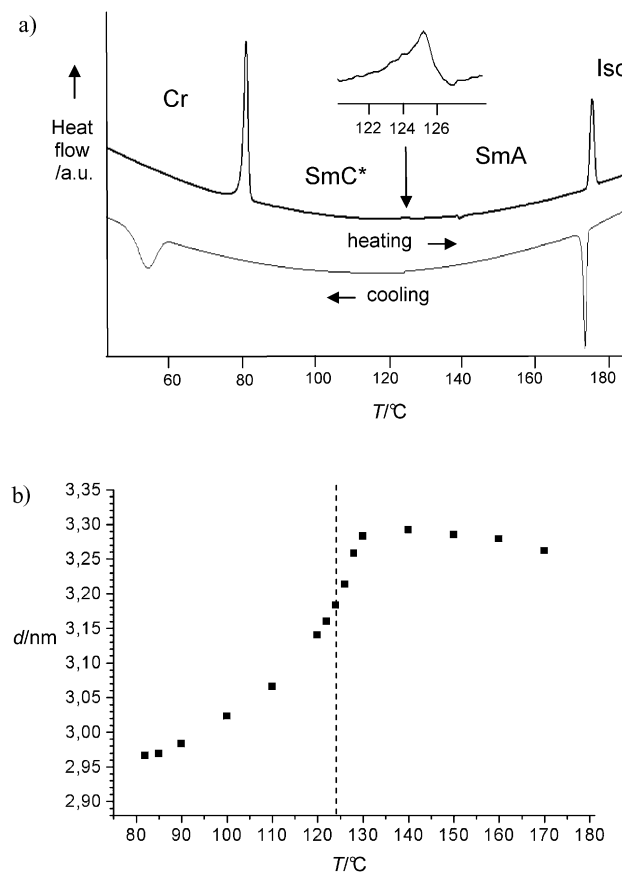
Compounds	R	$T^{\circ}\text{C}$ [ΔH kJ/mol]
8a	$-\text{C}_{10}\text{H}_{21}$	Cr 131 [42.3] (SmA 120 [6.1]) Iso
8b	$-(\text{CH}_2)_6\text{C}_4\text{F}_9$	Cr 122 [36.7] SmA 205 [10.1] Iso
8c	$-(\text{CH}_2)_4\text{C}_6\text{F}_{13}$	Cr 144 [37.8] SmA 223 [3.9] Iso

^a For conditions and abbreviations, see Table 1.**Fig. 1** Polarised light optical photomicrographs of the mesophases of **6c** as observed on cooling: (a) SmA phase at 146 °C; (b) SmC* phase at 110 °C and (c) SmC* phase at 83 °C (distinct region with Schlieren texture, magnification $\times 200$).

a Schlieren texture with exclusively four-brush disclinations is formed. In the regions of the fan texture these fans become broken. These textural changes indicate a transition from the SmA phase where the molecules are organized on average perpendicular to the layers to a tilted SmC* phase. The typical textures of the smectic mesophases of compound **6c** are shown in Fig. 1.

X-Ray investigations confirm layer structures for the mesophases of compound **6c**. The pattern of the smectic A phase shows two Bragg reflections in the small-angle region with d -value ratios of $1 : \frac{1}{2}$, corresponding to a layer distance of $d = 3.3$ nm (see Fig. 2b for temperature dependence). This d -value corresponds to the maximal possible molecular length of $L = 3.3$ nm as determined with CPK models,²⁰ assuming the most stretched conformation. As it is unlikely that the molecules adopt a strictly linear conformation in the LC state, it is assumed that the structure is composed of antiparallel pairs of molecules (see Fig. S5 in the ESI†) as in case of the related compound **9c**¹⁵ containing a hexyl chain at the N-substituted phenyl ring, the aliphatic and aromatic segments being completely intercalated with separate R_F sublayers and in these R_F layers there is only a partial intercalation of the R_F segments.

The 2D pattern of an aligned sample (Fig. 3a) displays the maxima of the diffuse outer scattering in a direction perpendicular to that of the layer reflections as expected for the SmA phase. The position of the outer diffuse scattering with respect to that of the layer reflections changes only slightly below the

**Fig. 2** Compound **6c**: a) DSC scan (first heating and first cooling); b) temperature dependence of the layer spacing d on heating (see Table S1 in the ESI,† dashed line indicates the SmC*-SmA phase transition region).

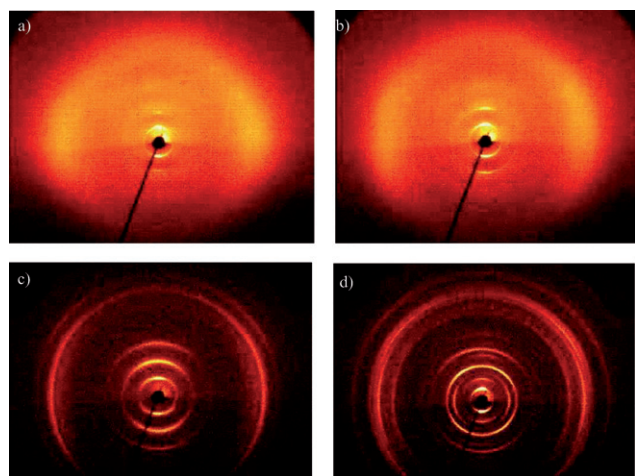


Fig. 3 2D X-ray diffraction patterns of a surface-aligned sample of **6c**: a) SmA phase at $T = 150\text{ }^{\circ}\text{C}$ on heating; b) SmC* phase at $T = 85\text{ }^{\circ}\text{C}$ on heating, c) monotropic crystalline layer phase at $T = 25\text{ }^{\circ}\text{C}$ as obtained upon rapid cooling from the isotropic liquid, d) crystalline phase at $T = 70\text{ }^{\circ}\text{C}$ on heating for comparison. The lower part of the patterns is shaded by the heating stage.

transition to the SmC* phase (see Fig. 3b), though the layer distance decreases significantly (see Fig. 2b) as typical for the onset of tilt which increases with decreasing temperature. As a consequence, the tilt angles derived from the positions for the maxima of the outer diffuse scattering are significantly smaller than those calculated from the layer spacings in the SmC* phase and those near the phase transition in the SmA phase by $\cos(\tau_{\text{calc}}) = d(\text{SmC}^*)/d(\text{SmA})$ (see Table S2 and Fig. S4 in the ESI†), which might be explained as follows. The maximum of the diffuse wide angle scattering is between $d = 0.54\text{ nm}$ at $170\text{ }^{\circ}\text{C}$ and $d = 0.50\text{ nm}$ at $85\text{ }^{\circ}\text{C}$, which means that it is mainly determined by the mean distance between the R_{F} chains (highest electron density) and hence the tilt of the aromatic and aliphatic parts (weaker scatterer) could in fact be stronger than actually recognized in the diffraction patterns. Electrooptical investigations (see Fig. S1 in the ESI†) indicate a polar switching at $T < 125\text{ }^{\circ}\text{C}$ which is also in line with the proposed SmA-to-SmC* transition.

Compound **6c** forms a monotropic (metastable) crystalline phase on rapidly cooling from the isotropic liquid to ambient temperature. Judging from the 2D X-ray pattern at $25\text{ }^{\circ}\text{C}$ showing layer reflections of the first to the third order and

a number of sharp reflections in the wide-angle region (see Fig. 3c and Table S1 and Fig. S3 in the ESI†) it is assumed to be composed of layers with a spacing of 2.72 nm exhibiting long-range molecular order in the layers but also a comparatively high degree of disorder indicated by the diffuse part of the wide-angle scattering. On heating, this phase transforms to a conventional crystalline phase showing Bragg reflections in the whole scattering range (see Fig. 3d and Fig. S3 in the ESI†).

A comparison of the phase transition data for the semi-fluorinated chiral salicylaldimines **6a–c** with the related compounds **9a–c**¹⁵ containing a hexyl chain at the N-substituted phenyl rings (see Fig. 4) shows that the kind of side chain plays a determining role in the formation of the liquid crystalline phases. The clearing points of salicylaldimine **6a** and semi-fluorinated analogues **6b** and **6c** decrease compared to the compounds with hexyl chains **9a**, **9b** and **9c**, whereas the melting points increase. Hence, the salicylaldimines **6** show mesophase intervals about $14\text{--}18\text{ }^{\circ}\text{C}$ narrower than the related compounds with hexyl chains **9**. Nevertheless, the SmC* ranges are often broader in the series of compounds **6**. In this series there is also a pronounced effect on the SmC* phase stability which rises with increasing degree of fluorination.

Mesomorphic properties of imine compounds 7. Compound **7a**, which was described in the literature,¹⁸ shows monotropic SmA and SmC* mesophases with fingerprint and broken fan textures, respectively. Both chiral imine compounds with semifluorinated alkyl chains **7b** and **7c** exhibit an enantiotropic smectic A phase. On cooling compound **7b**, with only 9 fluorine atoms in the semifluorinated side chain, a transition to a monotropic SmC* phase takes place at $99\text{ }^{\circ}\text{C}$, as seen by the formation of a Schlieren texture in the homeotropic regions of the SmA phase. For compound **7c** with an increased degree of fluorination (13 fluorine atoms in the semifluorinated side chain), the transition temperatures were further increased and the smectic C* phase was stabilized and becomes enantiotropic and in addition a monotropic mesophase (SmX*) occurs below this smectic C* phase. The transition from SmC* to SmX* is associated with a colour change in the broken fan-shaped texture (see Fig. 5b, c). X-Ray investigations on compound **7c** confirm a layer structure with $d = 3.24\text{ nm}$ at $130\text{ }^{\circ}\text{C}$ (SmA) and $d = 2.96\text{ nm}$ at $90\text{ }^{\circ}\text{C}$ (SmC*) which are very similar to the layer spacings observed for the related salicylaldimine **6c** with the same molecular length. Hence, the models of the organization in the SmA and SmC*

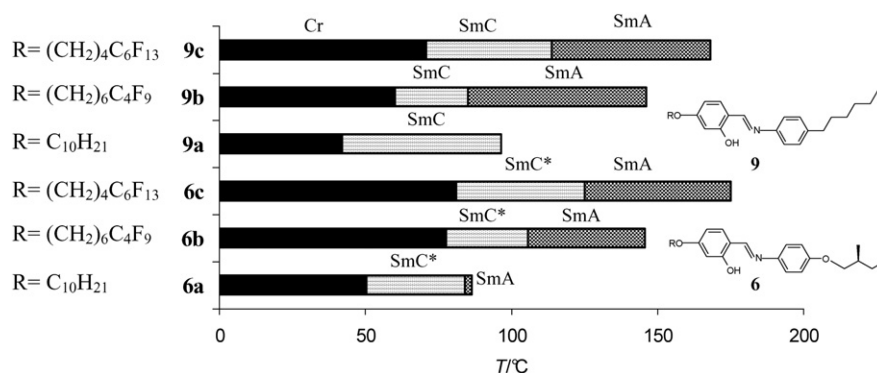


Fig. 4 Comparison of the mesomorphic behaviour of compounds **6** with that of the hexyl substituted compounds **9**.¹⁵

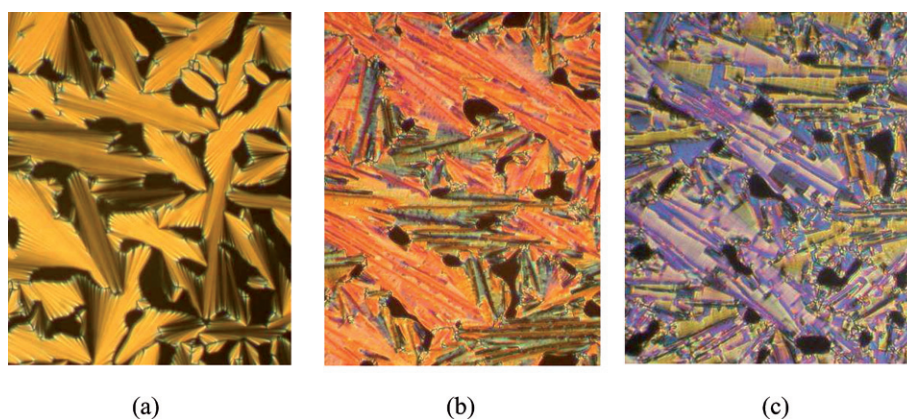


Fig. 5 Polarised light optical photomicrographs of the mesophases of **7c** as observed on cooling: (a) smectic A phase at 136 °C; (b) smectic C* phase at 110 °C; (c) SmX* phase at 65 °C (magnification $\times 200$).

phases of compound **6c** can also be applied here. At lower temperature the samples crystallize, so that the SmX* phase could not be investigated in more detail. The clearing points and mesophase ranges of the imine compounds **7a** to **7c** increase with increasing number of fluorine atoms within the terminal alkyl chain leading to a stabilisation of smectic mesophases.

A comparison of the mesomorphic properties of the salicylaldimines **6a–c** and the related imines **7a–c** (see Fig. 6) shows that there is a greater mesophase stability for the salicylaldimines because of the presence of a lateral hydroxy group which can affect the rigidity and polarisability of the mesogenic aromatic core due to intramolecular hydrogen bonding.^{17a,21} The additional OH group also increases the polarity of the core region and enhances the incompatibility with the non-polar chains which contributes to a compensation of the steric distortion provided by the lateral OH group. Intermolecular hydrogen bonding and dipolar interactions could also contribute to this effect.

Mesomorphic properties of copper(II) complexes 8. In order to examine the influence of fluorination on the bidentate salicylaldimato copper(II) complexes, a series of compounds **8** bearing a chiral and a semiperfluorinated chain were synthesized. The phase transition temperatures and enthalpies of these complexes **8** are given in Table 2. All of the mononuclear complexes **8** exhibit smectic A phases with typical fan-shaped texture (see Fig. S2 in ESI†), which can be aligned homeotropically. The

fluorolkylated metallomesogens **8b** and **8c** exhibit enantiotropic smectic A phases whereas the mesophase of the hydrocarbon analog **8a** is only monotropic. Increasing the number of fluorine atoms in the fluoroalkyl chain leads to a stabilisation of smectic mesophases, hence the semifluorinated metallomesogens **8b** and **8c** exhibit relatively high clearing points accompanied by partial decomposition. The layer distance in the SmA phase of compound **8b**, for example, is $d = 3.1$ nm (see Table S1 in the ESI†), indicating that the model of organization suggested for ligands **6c** and **7c** can also be applied to the organization of the Cu(II) complexes in the SmA phases. The loss of tilt (no transition to SmC*) could probably be due to the fact that complexation with Cu(II) increases the space required by the rigid core structure and therefore space filling in these regions is achieved without tilting of the aromatics.

Comparing the complexes **8** with their ligands **6** indicates an increase of the transition temperatures by metal coordination by about 34 to 61 K. This might largely be due to the increased polarizability of the Cu complexes and the preorganization of the rod-like cores by dimerization *via* metal coordination.

Fig. 7 gives a graphical overview of the behaviour of the branched copper(II) complexes **8** and compounds **10** with *n*-hexyl chains.¹⁵ The melting and clearing points and also the mesophase range of the non-fluorinated copper complex **8a** are similar to those of **10a**, but for the complex **8a** the smectic phase is only monotropic, whereas it is enantiotropic for **10a**.

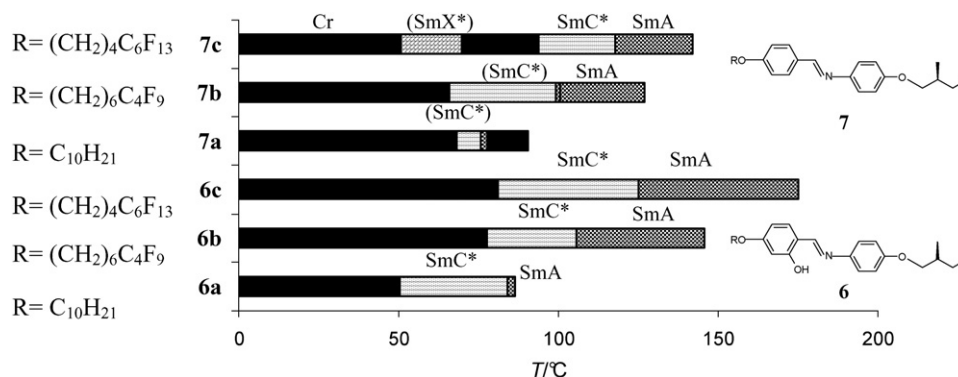


Fig. 6 Comparison of the thermal behaviour of compounds **6** and **7**.

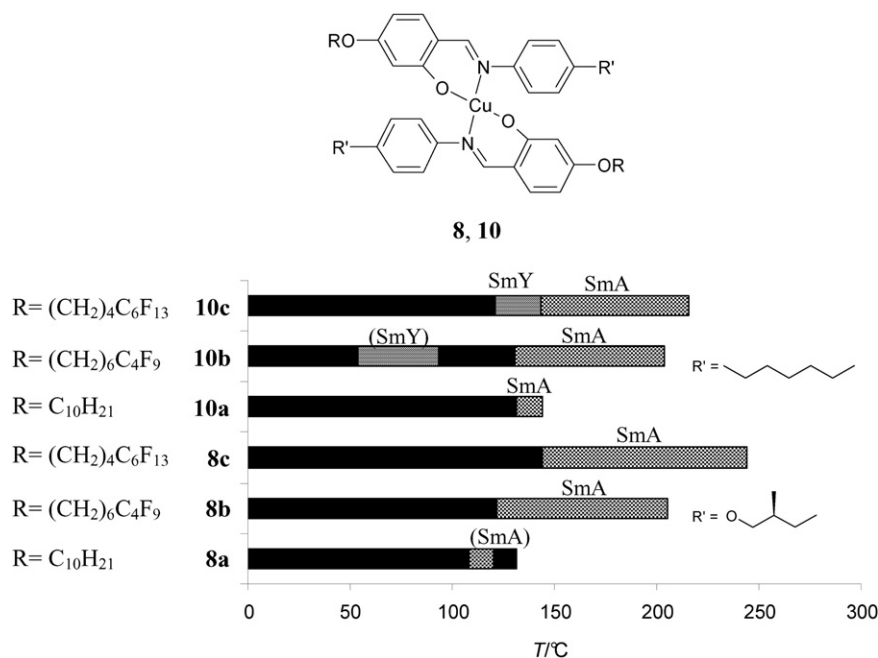


Fig. 7 Comparison of the thermal behaviour of the copper(II) complexes **8** and **10** (SmY = low temperature smectic phase with unknown structure).¹⁵

The mesophase ranges of the semifluorinated complexes **8b** and **8c** are slightly broader than those of the hexyl substituted complexes **10b** and **10c**, whereas the melting points are nearly the same. Overall, in the series of the chiral compounds **8** with relatively short and branched alkyl chains there is a stronger influence of the degree of fluorination on the mesophase stability compared to the related compounds **10** with longer linear alkyl chains.

3. Conclusion

We have prepared two new series of semiperfluorinated imine compounds containing a chiral side chain and investigated their mesomorphic properties in detail. The general trends observed for the liquid crystalline phases of the compounds, depending on the molecular structure, are summarised in Fig. 6 and 7.

The introduction of perfluoroalkyl chains leads to a stabilization of smectic liquid crystalline phases. Not only is the mesophase stability increased by the R_F chains, but also the temperature range of the smectic A and smectic C* phases becomes wider with increasing degree of fluorination. The complexation of the salicylaldehyde ligands **6** with copper(II) gives rise to new mesogenic materials combining chirality and the fluorophobic effect with metal centres in the mesogens. While the ligands show a polymorphism of different smectic phases, all copper complexes form only a SmA phase. Compared to the analogous hydrocarbon complexes the semiperfluorinated metallomesogens **8** have a significantly increased mesophase stability and exhibit wider mesomorphic temperature ranges.

Acknowledgements

B. Bilgin-Eran is grateful to the Alexander von Humboldt Foundation, for a research fellowship at Universität Halle-Wittenberg, Halle, Germany. This research has been supported

by Yildiz Technical University Scientific Research Projects Coordination Department. Project Number: 24-01-02-03.

References

- (a) P. Kirsch and M. Bremer, *Angew. Chem. Int. Ed.*, 2000, **39**, 4216; (b) K. Johns and G. Stead, *J. Fluorine Chem.*, 2000, **104**, 5; (c) H.-J. Lehmler, M. O. Oyewumi, M. Jay and P. M. Bummer, *J. Fluorine Chem.*, 2001, **107**, 141; (d) X. Li, L. Andruzzi, E. Chiellini, G. Galli, C. K. Ober, A. Hexemer, E. J. Kramer and D. A. Fischer, *Macromolecules*, 2002, **35**, 8078; (e) M. Yoneya, E. Nishikawa and H. Yokoyama, *J. Chem. Phys.*, 2004, **121**, 7520.
- (a) X.-H. Liu, I. Manners and D. W. Bruce, *J. Mater. Chem.*, 1998, **8**, 1555; (b) F. Guittard, E. T. de Givenchy, S. Geribaldi and A. Cambon, *J. Fluorine Chem.*, 1999, **100**, 85; (c) F. Guittard and S. Geribaldi, *J. Fluorine Chem.*, 2001, **107**, 363.
- M. Hird, J. W. Goodby, R. A. Lewis and K. J. Toyne, *Mol. Cryst. Liq. Cryst.*, 2003, **401**(1), 115; M. Hird, *Chem. Soc. Rev.*, 2007, **36**, 2070.
- (a) A. Schaz and G. Lattermann, *Liq. Cryst.*, 2005, **32**, 407; (b) A. Schaz, E. Valaityte and G. Lattermann, *Liq. Cryst.*, 2005, **32**, 513.
- (a) Y.-G. Yang, B.-Q. Chen and J.-X. Wen, *Liq. Cryst.*, 1999, **26**, 893; (b) K. Wang, H. Li, K. Liu and J.-X. Wen, *Liq. Cryst.*, 2001, **28**, 1573.
- (a) C. Tschierske, *J. Mater. Chem.*, 1998, **8**, 1485; (b) C. Tschierske, *J. Mater. Chem.*, 2001, **11**, 2647.
- (a) A. Pegenau, X. H. Cheng, C. Tschierske, P. Göring and S. Diele, *New J. Chem.*, 1999, **23**, 465; (b) X. H. Cheng, S. Diele and C. Tschierske, *Angew. Chem. Int. Ed.*, 2000, **39**, 592.
- (a) X. H. Cheng, M. K. Das, S. Diele and C. Tschierske, *Langmuir*, 2002, **18**, 6521; (b) X. H. Cheng, M. Prehm, M. K. Das, J. Kain, U. Baumeister, S. Diele, D. Leine, A. Blume and C. Tschierske, *J. Am. Chem. Soc.*, 2003, **125**, 10977.
- (a) B. Bilgin-Eran, C. Tschierske, S. Diele and U. Baumeister, *J. Mater. Chem.*, 2006, **16**, 1136; (b) B. Bilgin-Eran, C. Tschierske, S. Diele and U. Baumeister, *J. Mater. Chem.*, 2006, **16**, 1145.
- (a) M.-A. Guillevic and D. W. Bruce, *Liq. Cryst.*, 2000, **27**, 153; (b) M.-A. Guillevic, T. Gelbrich, M. B. Hursthouse and D. W. Bruce, *Mol. Cryst. Liq. Cryst.*, 2001, **362**, 147; (c) J. Szydłowska, A. Krowczyński, U. Pietrasik and A. Rogowska, *Liq. Cryst.*, 2005, **32**, 651; (d) R. Dembinski, P. Spinet, S. Lentijo, M. W. Markowicz, J. M. Martin-Alvarez, A. L. Rheingold, D. J. Schmidt and A. Sniady, *Eur. J. Inorg. Chem.*, 2008, **10**, 1565; (e) A. Głębowska, P. Przybylski, M. Winek, P. Krzyczkowska, A. Krowczyński,

- J. Szydłowska, D. Pocięcha and E. Gorecka, *J. Mater. Chem.*, 2009, **19**, 1395–1398.
- 11 G. Johansson, V. Percec, G. Ungarn and J. P. Zhou, *Macromolecules*, 1996, **29**, 646.
- 12 J. P. F. Lagerwall, A. Saipa, F. Giesselmann and R. Dabrowski, *Liq. Cryst.*, 2004, **31**, 1175–1184.
- 13 J. P. F. Lagerwall and F. Giesselmann, *Chem. Phys. Chem.*, 2006, **7**, 20–45.
- 14 (a) H.-S. Kitzerow, C. Bahr, *Chirality in Liquid Crystals*, Springer, New York, 2001; (b) H. Liu and H. Nohira, *Liq. Cryst.*, 1998, **24**, 719; (c) P. Pinol, M. B. Ros, J. L. Serrano, T. Sierra and M. R. de la Fuente, *Liq. Cryst.*, 2004, **31**, 1293.
- 15 B. Bilgin-Eran, C. Yorur, C. Tschierske, M. Prehm and U. Baumeister, *J. Mater. Chem.*, 2007, **17**, 2319.
- 16 (a) J. L. Serrano, *Metallomesogens*, VCH, Weinheim 1996; (b) B. Donnio, D. Guillon, R. Deschenaux and D. W. Bruce, *Comprehensive Coordination Chemistry II*, 2004, **7**, 357–627.
- 17 (a) B. Otterholm, M. Nilsson, S. T. Lagerwall and K. Skarp, *Liq. Cryst.*, 1987, **2**, 757; (b) B. Bilgin Eran, D. Singer and K. Praefcke, *Eur. J. Inorg. Chem.*, 2001, 111.
- 18 J. Barbera, E. Melendez, J. L. Serrano, M. T. Sierra, A. Ezcurra and M. A. Perez Jubindo, *Mol. Cryst. Liq. Cryst.*, 1989, **170**, 151.
- 19 (a) M. Marcos, P. Romero and J. L. Serrano, *Chem. Mater.*, 1990, **2**, 495; (b) M. Marcos, P. Romero, J. L. Serrano, J. Barbera and A. M. Levelut, *Liq. Cryst.*, 1990, **7**, 251; (c) F. R. Diaz, N. Valdebenito, J. L. Serrano, M. Marcos, J. I. Martinez and P. J. Alonso, *Liq. Cryst.*, 1998, **25**, 217.
- 20 Space-filling models (also known as calotte models or CPK models by Corey, Pauling and Koltun), see R. B. Corey and L. Pauling, *Rev. Sci. Instr.*, 1953, **24**, 621–627.
- 21 D. Lopez de Murillas, R. Pinol, M. B. Ros, J. L. Serrano, T. Sierra and M. Rosario de la Fuente, *J. Mater. Chem.*, 2004, **14**, 1117.